Atmos. Chem. Phys. Discuss., https://doi.org/10.5194/acp-2017-1103
Manuscript under review for journal Atmos. Chem. Phys.
Discussion started: 9 January 2018

Atmospheric Chemistry and Physics Discussions

The $\Delta^{17}O$ and $\delta^{18}O$ values of simultaneously collected atmospheric nitrates from anthropogenic sources – Implications for polluted air masses

Martine M. Savard[1*], Amanda Cole[2], Robert Vet[2], Anna Smirnoff[1]

[1] Geological Survey of Canada (Natural Resources Canada), 490 de la Couronne, Québec (QC), G1K 9A9, Canada
[2] Air Quality Research Division, Environment and Climate Change Canada, 4905 Dufferin St., Toronto (ON), M3H 5T4, Canada

Correspondence to: Martine M. Savard (martinem.savard@canada.ca)

Abstract. There are clear motivations for better understanding the atmospheric processes that transform nitrogen (N) oxides (NO_x) emitted from anthropogenic sources into nitrates (NO_3^-), two of them being that NO_3^- contributes to acidification and eutrophication of terrestrial and aquatic ecosystems, and particulate nitrate may play a role in climate dynamics. For these reasons, oxygen isotope ratios ($\delta^{18}O$, $\Delta^{17}O$) have been applied to infer the chemical pathways leading to the observed distribution of wet (w-NO_3^-), particulate (p- NO_3^-), and the sum of p-NO_3^- and gaseous HNO_3, while the gaseous form (HNO_3) has never been separately characterized for ^{17}O. Previous research studies have investigated w-NO_3^-, p-NO_3^- or p-NO_3^- + HNO_3 from non-polluted or polluted air masses, and inferred seasonal changes in the dominance of oxidation pathways to account for higher $\delta^{18}O$ and $\Delta^{17}O$ values in winter relative to summer. However, none of the polluted air studies collected samples specific to targeted emission sources. Here we have used a wind-sector-based, multi-stage filter sampling system and precipitation collector to simultaneously sample HNO_3 and p-NO_3^-, and co-collect w-NO_3^-, downwind from five different anthropogenic sources.

Overall, the w- and p-NO_3 $\delta^{18}O$ and $\Delta^{17}O$ values show expected differences between cold and warm seasons, but only the $\Delta^{17}O$ values of HNO_3 follow this pattern. The HNO_3 $\delta^{18}O$ ranges are distinct from the w- and p-NO_3^- patterns. Interestingly, the $\Delta^{17}O$ differences between p-NO_3^- and HNO_3 shifts from positive during cold sampling periods to negative during warm periods. The summer pattern may be due to the presence of nitrates derived from NO_x that has not yet reached isotopic equilibrium with O_3 and subsequent differences in dry deposition rates, while the larger proportion of p-NO_3^- formed *via* the N_2O_5 pathway can explain the fall-winter pattern. Very low p-NO_3^- $\Delta^{17}O$ values observed during warm months may be due to this non-equilibrated NO_x, though contribution from RO_2 oxidation remains a possibility. Our results show that the isotopic signals of HNO_3, w-NO_3^- and p-NO_3^- are not interchangeable and that their differences can further our understanding of NO_x oxidation and deposition. Future research should investigate all tropospheric nitrate species as well as NO_x to refine our understanding of nitrate worldwide and to develop effective emission reduction strategies.

Atmos. Chem. Phys. Discuss., https://doi.org/10.5194/acp-2017-1103
Manuscript under review for journal Atmos. Chem. Phys.
Discussion started: 9 January 2018

Atmospheric Chemistry and Physics Discussions

1 Introduction

Anthropogenic NO_x (NO and NO_2) emissions are oxidized to nitrate in the atmosphere in the form of gaseous (HNO_3), wet (precipitation or w-NO_3^-) or particulate (p-NO_3^-) forms, HNO_3 being one of the main precursors of p-NO_3^-. All these species may have detrimental effects on human health and aquatic and terrestrial ecosystems through inhalation, acidification and excess nitrogen deposition. In addition, aerosols may play a significant role in regional climate dynamics as they interact with clouds and solar radiation (e.g., IPCC, 2013). For these reasons, understanding the chemical processes controlling the transport and fate of atmospheric reactive N is required to help develop effective emission reduction strategies and drive climate models (in the present article, we use *nitrates* to refer to p-NO_3, HNO_3 and w-NO_3 together).

Triple oxygen isotopes ($\delta^{18}O$ and $\delta^{17}O$) may serve for deciphering atmospheric oxidation pathways of NO_x leading to ambient nitrate. Michalski et al. (2003) performed the first measurement of $\delta^{17}O$ values in atmospheric nitrate. The authors found that atmospheric nitrate is highly enriched in ^{18}O and ^{17}O, likely due to the transfer of anomalous oxygen atoms from ozone (O_3) via the NO_x-ozone photochemical cycle and oxidation to nitrate. During its formation, O_3 inherits abnormally high $\delta^{18}O$ and $\delta^{17}O$ values through mass independent fractionation. The specific $\delta^{17}O$ departure from the terrestrial mass dependent fractionation line, named ^{17}O anomaly, is expressed as $\Delta^{17}O = \delta^{17}O - 0.517 \times \delta^{18}O$ (Thiemens, 1999). Further investigations suggested that the $\delta^{18}O$ and $\delta^{17}O$ values of w-NO_3^- and p-NO_3^- reflect several reactions taking place after the atmospheric emission of NO_x, *i.e.*, atmospheric oxidation pathways transforming NO_x into secondary products (Hastings et al., 2003; Michalski et al., 2003; Michalski et al., 2004; Morin et al., 2007; Savarino et al., 2007; Alexander et al., 2009). Seasonal $\delta^{18}O$ differences in w-NO_3^- samples (less variable and lower values during summer) have been interpreted to be due to changes in these chemical pathways (Hastings et al., 2003). Modeling and validation based on sparse existing data provide hope regarding a global understanding of atmospheric nitrate (Alexander et al., 2009), and further measurements need to be done on the ground, particularly at mid-latitudes.

Additional studies dealing with triple oxygen isotope characterizations have addressed questions of methodology (Kaiser et al., 2007; Smirnoff et al., 2012), transfer of the ozone ^{17}O anomaly to atmospheric nitrate (Liang and Yung, 2007; Savarino et al., 2008; Michalski et al., 2014), or sources and chemical pathways of high (Arctic) and low (Taiwan) latitude nitrate (Morin et al., 2008; Guha et al., 2017, respectively). Triple oxygen isotope characterizations of field NO_3^- samples are not yet widespread. The few existing studies have chiefly characterized w-NO_3^- or the sum of p-NO_3^- and HNO_3 (Michalski et al., 2004; Morin et al., 2007; Morin et al., 2008; Alexander et al., 2009; Morin et al., 2009; Proemse et al., 2012; Guha et al., 2017), and suggested these indicators would be useful to trace atmospheric nitrate in water (Kendall et al., 2007; Tsunogai et al., 2010; Dahal and Hastings, 2016). Elliott et al. (2009) measured $\delta^{18}O$, but not $\Delta^{17}O$, in United States CASTNET (Clean Air Status and Trends Network) samples of simultaneously-collected p-NO_3^- and HNO_3 as well as in nearby NTN (National Trends Network) precipitation samples. Even rarer are the nitrate $\delta^{18}O$ and $\Delta^{17}O$ values of field samples downwind from NO_x-emitting sources at mid-latitudes (Kendall et al., 2007; Proemse et al., 2013). In those studies, $\delta^{18}O$ and $\Delta^{17}O$ values were suggested to be useful to apportion the contribution of emission sources to regional atmospheric nitrate loads. However, the signals of precursor NO_x emitted from the same sources may quickly get modified through isotopic equilibration with O_3, so that the original source signals may be difficult to recognize.

Atmos. Chem. Phys. Discuss., https://doi.org/10.5194/acp-2017-1103
Manuscript under review for journal Atmos. Chem. Phys.
Discussion started: 9 January 2018

Atmospheric Chemistry and Physics Discussions

In the past, due to sampling challenges, HNO_3 and p-NO_3^- were generally collected together (without differentiation). Therefore, no studies have separately and simultaneously collected and analyzed the HNO_3 and p-NO_3^- $\delta^{18}O$ and $\Delta^{17}O$ values, and discussed these isotopic characteristics of nitrate collected downwind of anthropogenic emitters at mid-latitudes. It is clear that investigating the causes of isotopic fractionation of these nitrate species and identifying the reaction pathways responsible for their transformation would contribute to our understanding of nitrogen worldwide.

While national reported NO_x emissions in Canada declined steadily from 2000 to 2015, emissions in the Province of Alberta have remained relatively constant since 2004 (Environment and Climate Change Canada, 2016). Pioneering work was accomplished measuring nitrate on emitted PM2.5 (particulate matter less than 2.5 µm) and in bulk and throughfall precipitation samples (wet and some dry deposition on ion exchange resin collectors) collected at or downwind of the Athabasca oil-sands mining operations in Alberta (Proemse et al., 2012; Proemse et al., 2013). However, the Edmonton area in Central Alberta, known to generate the highest NO_x emissions in Canada, and the area of southern Alberta, characterized by dense gas compressor station and agricultural emissions, have never been investigated.

Here we have characterized nitrate downwind of five targeted emission sources in central and southern Alberta, namely: (1) coal-fired power plants, (2) city traffic, (3) chemical industries and metal refining, (4) fertilizer plant and oil refinery, and (5) gas compressors plus cattle and swine feedlots. To this end, we employed wind-sector-based active samplers to collect HNO_3 and p-NO_3^- as well as w-NO_3^- downwind of the source types. The objective of this work was to assess the atmospheric NO_x reaction pathways and processes responsible for the distribution of HNO_3, and w- and p-NO_3^- in mid-latitudinal regions.

2 Methodology

2.1 Regional context

This research project investigated nitrates (p-NO_3^-, HNO_3 and w-NO_3^-) from three main emission source areas: the Genesee and Edmonton areas of central Alberta, and the Vauxhall area of southern Alberta. These areas experience a continental climate, but the mean annual temperature at Vauxhall is slightly higher (5.6 °C) and total annual precipitation lower (320 mm) than in central Alberta (3.9°C; 537 mm; Fig. SI-1). Autumn is generally the wettest season and winter the driest. The sampling sites were at altitudes between 645 and 820 m (altitude above sea level), and in continental regions devoid of the influence of marine air masses (negligible halogen oxides).

The rural Vauxhall area was selected for collecting nitrates emitted from multiple small gas compressor stations scattered throughout southern Alberta and reduced N from cattle and swine feedlots (see Savard et al., 2017). The other anthropogenic emissions are from three sites in central Alberta: coal-fired power plants (CFPP) at the Genesee site, 55 km southwest of Edmonton; traffic-dominated emissions at Terrace Heights, a residential area near downtown Edmonton; and an industrial area in Fort Saskatchewan, northeast of Edmonton, where sampling two different wind sectors allowed separating different industries. In Fort Saskatchewan, sampling in the northwest sector targeted emissions from a mixture of sources of which the

Atmos. Chem. Phys. Discuss., https://doi.org/10.5194/acp-2017-1103
Manuscript under review for journal Atmos. Chem. Phys.
Discussion started: 9 January 2018

largest were a chemical plant and metal refinery (referred to as chemical plus metal industries), while the north sector point emissions were dominated by a fertilizer plant and an oil refinery (referred to as fertilizers plus oil).

2.2 Sampling protocols

Collection of nitrate samples took place between 30 September 2010 and 20 January 2014. Active air sampling was carried out using a modified version of Environment Canada's standard CAPMoN (Canadian Air and Precipitation Monitoring Network) sampling protocol, which is recognized and used worldwide to measure ambient NO_3^- (HNO_3 and p-NO_3^-). A description of the samplers and sample handling protocols is available in the literature (Sirois and Vet, 1999). A 'conditional sampling' method was employed to maximize the collection of nitrogen compounds from the sources of interest, in which the sampling pumps and precipitation collector were activated when the site wind vane registered winds from the direction of the targeted sources. The CAPMoN sampling system was installed and operated at different sites, each at varying distances from the targeted point (<1 to 25 km), and diffuse sources (3 to >125 km; Table 1). Back trajectories run using the HYSPLIT model (Stein et al., 2015; Rolph, 2017) for every hour of sampling verified that very few air masses within the sampling sector passed over other sources outside of the targeted ones in the preceding 24 hours. Ambient air was pulled through a three-stage filterpack system to collect, sequentially, particulate matter, gaseous nitric acid (HNO_3), and gaseous ammonia (NH_3; see (Savard et al., 2017), for exact location of sampling sites and $\delta^{15}N$ values of reduced and oxidized atmospheric N species). Here we report on the simultaneously sampled HNO_3 and p-NO_3^-, along with co-sampled w-NO_3^- in rain and snow samples collected in CAPMoN wet-only precipitation samplers. Note that precipitation events did not occur regularly (see Fig. SI 1), so that the number of aqueous samples collected was fewer than the gas and particulate samples. Both the air and precipitation samplers were only active when the wind direction was from the desired source sector and the wind speed was greater than 0.55 m/s. Four identical air-sampling systems operated simultaneously at each site, with samples pooled when necessary to provide sufficient filter loadings for isotope analysis and, when possible, measured separately to estimate sampling precision. In contrast to the four gas-and-particle sampling systems, there was a single precipitation collector at each site, and therefore precision was not determined for precipitation samples. Individual sample deployment times ranged from 5 to 113 days, and total air sampling time within the wind-direction sectors ranged from 21 to 360 hours. The variable cumulative periods reflected the frequency of the wind flow from the targeted source sectors and the amount of time required to obtain sufficient mass loadings on the filters.

Two or three replicate samples for most species were pooled at Genesee and Vauxhall, the first two sampling sites, subject to the requirement that sampled air volumes be within 15 % of each other, thereby eliminating samples that experienced flow problems. At the sites sampled later in the Edmonton area, improvements to the laboratory analytical procedure allowed for smaller sample amounts and eliminated the need for sample pooling. Replicate isotopic values at these sites could be determined by analyzing each of the four samples individually.

Atmos. Chem. Phys. Discuss., https://doi.org/10.5194/acp-2017-1103
Manuscript under review for journal Atmos. Chem. Phys.
Discussion started: 9 January 2018

Atmospheric Chemistry and Physics Discussions

2.3 Analytical procedures

We characterized the triple oxygen isotopic ratios ($\delta^{17}O$, $\delta^{18}O$) of HNO_3, w-NO_3^-, and p-NO_3^-, along with their $\delta^{15}N$ values, and those of NH_3, w-NH_4, p-NH_4 and NO_x (all N isotopic results are in Savard et al., 2017). The present article deals solely with the $\delta^{18}O$ and $\delta^{17}O$ ($\Delta^{17}O$) values obtained for the three nitrate species. We treated the samples with the chemical conversion and thermal decomposition of N_2O protocols, providing the ability to simultaneously analyze low-concentration N- and O-containing species (Smirnoff et al., 2012).

A notable challenge in the analysis of the filter-based atmospheric samples is their small extraction volumes; only 6-10 mL of extract solution was normally available for the measurement of concentrations and isotopic analysis. In addition, concentrations of these low volume samples were generally low (7.1-21.4 NO_3 µmol/L) for the protocols preconized here. Therefore, not all samples could be diluted to produce volumes sufficient for reduction of NO_3^- to NO_2 and subsequent conversion to N_2O, the final product before isotope analysis. Samples with an initial concentration below (2.3 µmol/L) could not be treated, and some were combined to produce volumes sufficient for analyses (same sampling period but combination of several collected samples). All extracted N_2O was analyzed with the pre-concentration/gold furnace-IRMS system developed at the Geological Survey of Canada (Smirnoff et al., 2012). This approach allows the spectrum of $\delta^{15}N$, $\delta^{17}O$ and $\delta^{18}O$ ratios from O-bearing N-species to be determined in samples containing as little as 37.5 nmol of N (15 mL final solution). The USGS-34, USGS-35, USGS-32 nitrate reference materials were used and processed exactly the same way as the samples, *i.e.*, converted from nitrate to nitrite, then to N_2O. The laboratory analytical precision (average of replicates) determined during the present study using the described analytical procedures was 0.6 ‰ for $\delta^{18}O$ and $\delta^{17}O$ values in gaseous (n=12) and solid nitrates (n=20). For w-NO_3, analytical duplicates gave 0.6 and 0.5 ‰, for $\delta^{18}O$ (n=3) and $\delta^{17}O$ (n=4) values, respectively. The $\Delta^{17}O$ values are defined as $\ln(1+\delta^{17}O/1000) - 0.516 \times \ln(1+\delta^{18}O/1000)$, relative to Vienna Standard Mean Ocean (VSMOW).

3 Results and interpretation

3.1 Isotopic reproducibility when using the CAPMoN filterpack sampling system

Data obtained using at least two of the four identical CAPMoN sample collection streams at each sampling site were used to calculate the reproducibility of each isotopic value measured. With four or fewer samples collected during each sampling period, a non-parametric approach was deemed most appropriate. Therefore, for each period in which multiple (2-4) values were obtained, a median isotopic value was calculated, then the two to four absolute deviations from this median were calculated (Table 2). This operation was repeated for each of the 18 sampling periods in which multiple measurements were obtained. Although there were four replicates in 18 periods, the pooling of simultaneously collected samples and the QC steps described earlier reduced the total number of replicates for each compound (Table 3). The median absolute deviation (MAD) for each compound was then calculated from the 15-38 absolute deviations. Finally, the MAD was scaled by dividing by 0.6745 to give the modified median absolute deviation (M.MAD). This scaling factor ensures that the M.MAD will be consistent with the standard deviation in the event that the distribution is Gaussian (Randles and Wolfe, 1979; Sirois and Vet, 1999). This suite

Atmos. Chem. Phys. Discuss., https://doi.org/10.5194/acp-2017-1103
Manuscript under review for journal Atmos. Chem. Phys.
Discussion started: 9 January 2018

Atmospheric Chemistry and Physics Discussions

of parallel tests indicates that all measured species show coherent and reproducible $\delta^{18}O$ and $\delta^{17}O$ results, with the M.MAD varying between 0.7 and 2 ‰ (Table 2). These estimations encompass the precision of the entire method, including errors due to sampling, chemical treatments and instrumental analysis.

A potential complication of the air sampling method can arise if there was significant volatilization of NH_4NO_3 on the particle filter into HNO_3 and NH_3, with subsequent collection on the downstream gas filters. This could result in isotopic fractionation between the particle and gaseous components, which would become artificially high and low, respectively, with stronger effects at higher temperatures (summer) relative to lower temperatures (winter). We find the overall p-NO_3^- isotopic ratios to be higher during winter than during summer (see Section 3.4). Moreover, the p-NO_3^- minus HNO_3 isotopic difference is negative during summer, opposite to the expected isotopic artefact if particulate volatilization were influencing the final signal of the samples. We therefore concluded that collecting particles and gaseous components simultaneously provides the best information for understanding atmospheric reactive nitrogen. Finding that the sampling protocols are adequate for isotopic work is in agreement with a previous study using a comparable method that found minimal fractionation between p-NO_3^- and HNO_3 (Elliott et al., 2009).

3.2 Averages and ranges of triple oxygen isotopic results in Alberta

The average $\delta^{18}O$ and $\Delta^{17}O$ values of HNO_3 (gas), w- and p-NO_3^- show no apparent systematic ordering (Table 3), in contrast to what was found for $\delta^{15}N$ values in the same samples (Savard et al., 2017). In addition, there is no systematic tendency when looking at the samples collected downwind from the five-targeted sources: CFPP HNO_3 and p-NO_3^- have the highest $\delta^{18}O$ and $\Delta^{17}O$ averages, but not the highest w-NO_3^- values; chemical industries show the lowest $\delta^{18}O$ and $\Delta^{17}O$ averages for w- and p-NO_3, but not for HNO_3. At first sight, this observation suggests that the oxygen isotopes in the three nitrate species are not predominantly source-dependent (see Section 3.3).

Considering all nitrate species, the Alberta $\delta^{18}O$ and $\Delta^{17}O$ values range between +48.4 and +83.2 ‰, and between 13.8 and 30.5 ‰, respectively (Table 4). These ranges indicate that ozone partly transferred its isotopic anomaly to nitrates during NOx cycling and oxidation (nitrate derived through O_2 oxidation would show $\delta^{18}O$ and $\Delta^{17}O$ values of 23.5 and 0 ‰, respectively). When examining the existing $\delta^{18}O$ and $\Delta^{17}O$ data for w- and p-NO_3^- in the literature, the ranges for our mid-latitude samples are within those previously reported (Table 4). The worldwide compilation of documented data is broadening the $\delta^{18}O$ range of atmospheric NO_3^- previously suggested to be between 60 and 95 ‰ (Hastings et al., 2003; Kendall et al., 2007).

Previous studies that report triple isotope oxygen results in atmospheric NO_3 samples are scarce (Table 4). To our knowledge, triple oxygen isotopic characterization specific to HNO_3 has never been documented before; previous studies only reported values for the sum of HNO_3 and p-NO_3^- (Table 4). The HNO_3 range is within the broad spectrum of p-NO_3 values compiled for remote to contaminated sites. Elliott et al. (2009) have reported HNO_3 oxygen results for $\delta^{18}O$ values only, with a range of +51.6 to +94.0 ‰ (mean of 77.4), with simultaneously-sampled p-NO_3^- $\delta^{18}O$ values between +45.2 and +92.7 ‰ (mean of 75.2). Those ranges are broader than the HNO_3 and p-NO_3^- values obtained in the present study. The $\delta^{18}O$ and $\Delta^{17}O$ ranges we

Atmos. Chem. Phys. Discuss., https://doi.org/10.5194/acp-2017-1103
Manuscript under review for journal Atmos. Chem. Phys.
Discussion started: 9 January 2018

document here for HNO_3 in Alberta are narrower than those of the simultaneously collected p-NO_3^- (Fig. 1), suggesting that there are additional isotopic fractionation processes when HNO_3 is transformed to p-NO_3^-, or that p-NO_3 is derived from different pathways with more variation in isotopic signatures.

3.3 Covariations of $\Delta^{17}O$ and $\delta^{18}O$ values in nitrates from individual sources

The p-NO_3^-, w-NO_3^- and HNO_3 values co-vary when identified by source type in the $\delta^{18}O$ and $\Delta^{17}O$ space (Fig. 1). The isotopic range for a single source can be as large as 6 ‰ for $\Delta^{17}O$ values and 19 ‰ for $\delta^{18}O$ values in HNO_3, 12 and 17 ‰ in w-NO_3^-, and 7 and 21 ‰ in p-NO_3. Each source type clearly exhibits nitrate $\Delta^{17}O$ and $\delta^{18}O$ with a specific grouping. The CFPP w-NO_3^- results show a range similar to the HNO_3 results, but lower $\delta^{18}O$ values than the HNO_3 and p-NO_3^- groups. The few other precipitation samples show $\delta^{18}O$ and $\Delta^{17}O$ values generally higher than the p-NO_3^- and HNO_3 samples, again with exception of the chemical and metal industries.

The HNO_3 samples from a given source type tend to have a higher $\delta^{18}O$ value for a given $\Delta^{17}O$ value than p-NO_3^- (or *vice versa*; Fig. 1). These observations suggest that the contribution of oxidation pathways leading to HNO_3 and p-NO_3^- are not identical, or that there is an isotope fractionation in the conversion of HNO_3 to p-NO_3^-. Therefore, separate measurements of the gaseous and particle nitrate forms may provide additional constraints on oxidant concentrations.

Regarding the potential for identifying nitrate sources, it appears that using $\delta^{18}O$ and $\Delta^{17}O$ values for such a task is not feasible, as previously suggested in the literature (Michalski et al., 2003). This interpretation stems from the fact that nitrate species show either continuous trends regardless of their sources (p- and w- NO_3) or overlapping source results (HNO_3; Fig. 1).

The individual range of points identified by source may partly reflect different initial ambient conditions and rates of changes in ambient conditions during NO_x oxidation (Fig. 1; see Section 3.5). Specifically, each isotopic range may depict the progressively changing influence of ozone due to ambient conditions through time. Indeed, the atmospheric samples were collected repeatedly over several weeks or months at a given site (near a given source), and consecutively from one site to the other over more than three years; samples undeniably incorporate N-species produced under significantly changing ambient conditions.

3.4 Seasonal $\delta^{18}O$ and $\Delta^{17}O$ trends in nitrates

The $\Delta^{17}O$ and $\delta^{18}O$ results from all sources combined and identified by sampling period for HNO_3, w-NO_3^- and p-NO_3^- clearly show higher $\delta^{18}O$ and $\Delta^{17}O$ values during cold periods relative to warm periods (Fig. 2), with the exception of HNO_3 $\delta^{18}O$ values, which were similar in cold and warm periods. As mentioned above, the collection of several samples lasted over periods overlapping fall and winter periods and, in such cases, the results are labelled as covering the two seasons; note that for many fall cases, the average sampling temperatures were below 0°C. Nevertheless, plotting by sampling period can be regarded as a general repartition of results between warm and cold months, which show lower and higher isotopic values, respectively, in both the w- and p-NO_3^-.

Atmos. Chem. Phys. Discuss., https://doi.org/10.5194/acp-2017-1103
Manuscript under review for journal Atmos. Chem. Phys.
Discussion started: 9 January 2018

A series of reactions listed in Table 5 summarizes the main atmospheric processes taking place during the production of nitrates in contaminated air masses. First, during anthropogenic combustion of fossil fuels NO_x (NO and NO_2) is produced through reactions of air N_2 with atmospheric O_2 at high temperatures (reactions R1; Table 5). Then, NO_x cycles between NO and NO_2 through a series of reactions involving sunlight (R5), O_3 (R2, R4), and peroxy (HO_2) or alkyl peroxy (RO_2) radicals (R3; Morin et al., 2007; Fang et al., 2011; Michalski et al., 2014; here we use RO_2 to refer collectively to HO_2 and RO_2).

The oxidation of NO_x (specifically NO_2) to HNO_3 further incorporates additional O atoms from different oxidants (R6-R8; Table 5). Production of nitrate via R6 is restricted to daytime (since OH is generated through photochemistry), whereas production through reactions R4, R7 and R8 dominates at night. In addition, N_2O_5 is thermally unstable, so the p-NO_3^- contribution of the R4-R7-R8 pathway is larger during winter than during summer. We have neglected contributions from BrO cycling due to the location far from the coast, and from reactions of NO_3^- with hydrocarbons (R12) since they are predicted to have a minimal contribution to nitrate formation in this region (Alexander et al., 2009). Finally, HNO_3 in the gas phase can be irreversibly scavenged by wet surfaces or precipitation (R9) and calcium carbonate on particles (R11), and can equilibrate with solid ammonium nitrate where there is excess ammonia available (R10).

It has been previously suggested that the $\delta^{18}O$ and $\Delta^{17}O$ values of w- and p-NO_3^- formed during summer are lower than those during winter due to higher contribution from the N_2O_5 path (R4, R7-R8) during that season (e.g., Hastings et al., 2003; Morin et al., 2008). As an early take on the data identified by sampling periods, it seems that all the studied w- and p-NO_3^- show $\delta^{18}O$ and $\Delta^{17}O$ trends following the expected patterns for warm and cold months (Fig. 2). In the case of the less commonly studied HNO_3, the summer $\Delta^{17}O$ values are lower than the fall-winter, fall and spring ones, suggesting that the processes leading to the summer isotopic ratios perhaps include O_3 contributions similar to winter ones, but with lower $\Delta^{17}O$ values (see section 4.1).

3.5 Isotopic differences between HNO_3 and p-NO_3^-

Regarding the specific forms of nitrate, it is pertinent to mention that the HNO_3 concentrations (from 0.01 to 0.15 μg N/m^3; average of 0.06) are slightly lower than those of p-NO_3^- (from 0.02 to 0.35 μg N/m^3; average of 0.12). For context, the median concentrations at all CAPMoN sites, which represent non-urban areas across Canada, range from 0.07 to 1.1 μg N/m^3 for HNO_3 and from 0.03 to 2 μg N/m^3 for p-NO_3^- (Cheng and Zhang, 2017). In the Alberta samples, HNO_3 is present at such significant proportions, that if they had not been differentiated, the low end of the isotopic range obtained for p-NO_3^- would have been significantly higher in both $\delta^{18}O$ and $\Delta^{17}O$ (Table 4, see undifferentiated category). Hence, as far as the isotopic characteristics are concerned, an important feature to keep in mind is that the HNO_3 of central and southern Alberta has distinct properties relative to simultaneously-sampled p-NO_3^- and co-sampled w-NO_3^-. In practical terms, the relationships between the simultaneously sampled HNO_3 and p-NO_3^- are of four types (Fig. 3): (i) HNO_3 $\delta^{18}O$ and $\Delta^{17}O$ are both lower than p-NO_3^-; (ii) HNO_3 has lower $\Delta^{17}O$ but higher $\delta^{18}O$ values than p-NO_3^-; (iii) HNO_3 has higher $\delta^{18}O$ values and similar $\Delta^{17}O$ ones relative to p-NO_3^-; and (iv) HNO_3 has higher $\delta^{18}O$ and $\Delta^{17}O$ values than p-NO_3^- (Fig. 3).

Atmos. Chem. Phys. Discuss., https://doi.org/10.5194/acp-2017-1103
Manuscript under review for journal Atmos. Chem. Phys.
Discussion started: 9 January 2018

The fall-winter isotopic results belong to group (i), fall results, to groups (i), (ii) and (iii), and the spring and summer results, to groups (ii), (iii) and (iv). Elliott et al. (2009) reported simultaneously sampled p-NO_3^- and HNO_3 in northeastern USA with similar seasonal changes of $\delta^{18}O$ differences (no $\Delta^{17}O$ measurement). The HNO_3 $\delta^{18}O$ were generally similar or lower than the p-NO_3^- values during winter and fall, and slightly to much higher during spring and summer, with the spring and autumn p-NO_3^--HNO_3 relationships being roughly intermediate between the winter and summer ones. The average $\delta^{18}O$ difference of p-NO_3^- minus HNO_3 reported between winter and summer (15 ‰) by Elliott et al. (2009) agrees with the difference for fall-winter and summer obtained here (12 ‰).

The marked shifts in isotopic differences between the HNO_3 and p-NO_3^- reported here likely reflect changes in the dominant processes leading to the production of the different sampled nitrate forms (see Section 4.1). These isotopic differences also imply that the analysis of samples that combine p-NO_3^- and HNO_3 can mislead when attempting to understand in detail the chemical pathways involved in a specific region where HNO_3 is significantly present; and that the isotopic signals of HNO_3 and p-NO_3^- are not interchangeable in such cases.

4 Discussion

4.1 Dominant oxidation pathways producing HNO_3, w-NO_3^- and p-NO_3^-

The Alberta nitrate values do not fall on a single line but, rather, show a vertical extent in the $\delta^{18}O$ and $\Delta^{17}O$ space (Fig. 2) that exceeds the precision of the data (Section 2.3 and Table 2). This observation differs from several studies that measured bulk nitrate or a single nitrate species and reported $\delta^{18}O$ and $\Delta^{17}O$ sets as linear.

Considering the relevant oxidation reactions shown in Table 5, anthropogenic atmospheric nitrates incorporate O atoms from three main molecules, O_2 (via RO_2 - R3, and possibly source NO_x- R1), O_3 (via NO_2, NO_3^- and N_2O_5 – R2, R4, R7-R8) and H_2O (via OH, R5-R6). These molecules carry distinct isotopic signals that will partly determine the final $\delta^{18}O$ and $\Delta^{17}O$ values of the nitrate products. The $\delta^{18}O$ and $\Delta^{17}O$ values of O_2 are 23.5 and 0 ‰, respectively. Anthropogenic emitters involving combustion (O_2) may generate primary NO_x at or near sources that tend to carry low $\delta^{18}O$ and $\Delta^{17}O$ values. This primary NO_x (>90 % emitted as NO) cycles through NO-NO_2-O_3-NO numerous times before it is removed in R6. OH typically has negative $\delta^{18}O$ values and a $\Delta^{17}O$ value equal to 0 ‰ as it rapidly exchanges O isotopes with water vapour (Dubey et al., 1997; Röckmann et al., 1998). We obtained the average of precipitation $\delta^{18}O$ values for each sampling period at the studied sites (OPIC, 2017), and calculated the vapour signal using water-vapour fractionation factors (Clark and Fritz, 1997). Next, using fractionation factors between OH in equilibrium with H_2O vapour (Walters and Michalski, 2016), we calculated that the $\delta^{18}O$ values would range between -83 and -62 ‰. Peroxy radicals mostly derive from O_2 at mid latitudes (Michalski et al., 2003; Morin et al., 2007; Alexander et al., 2009), but they have a non-zero $\Delta^{17}O$ signal (1-2‰) due to the role of ozone in the HO_x cycle (Morin et al., 2011). However, their $\delta^{18}O$ values are difficult to measure, so they can only be inferred based on assumptions (+23.9 ‰; Fang et al., 2011; Guha et al., 2017). The $\delta^{18}O$ and $\Delta^{17}O$ values of bulk O_3 are generally between 90 and 120 ‰, and 30 and 34 ‰, respectively, but the transferable signals are suggested to be around 130 and 39 ‰ at mid-latitudes (Vicars and Savarino,

2014). Moreover, NO_x modelled at isotopic steady state with tropospheric O_3 yields 117 and 45 ‰ in $\delta^{18}O$ and $\Delta^{17}O$, respectively (Michalski et al., 2014). This neglects the contribution of NO oxidation by RO_2 (R3), which will reduce the steady-state $\Delta^{17}O$ and $\delta^{18}O$ of NO_x below the O_3-only oxidation value. The foregoing review of isotopic signals provides context to the interpretation of our data, keeping in mind that mass-dependent fractionation has likely played a role in determining nitrate $\delta^{18}O$ values.

Generally, the winter to summer isotopic differences are thought to be due to the high oxygen isotopic values of N_2O_5 due to interaction with O_3 (Johnston and Thiemens, 1997; Michalski et al., 2003; Morin et al., 2008; Vicars et al., 2012) and low values of OH in isotopic equilibrium with atmospheric H_2O (Dubey et al., 1997). According to Table 5, these two reaction pathways produce nitrates via R4-R7-R8 with 2/3 O from NO_2, 1/6 O from O_3 and 1/6 O from H_2O, and nitrates via R6 with 2 out of 3 O atoms coming from NO_2 and 1 added O from OH (e.g., Michalski et al., 2003). Using these proportions with the Alberta $\Delta^{17}O$ values of p-NO_3^- and HNO_3 in weighted averages allows us to make a rough estimation of the maximum and minimum $\Delta^{17}O$ values of NO_2 oxidized to nitrates in the air masses sampled. The calculations assume the O from O_3 contributes a signal of ~39 ‰ as was recently measured (Vicars et al., 2014) and that $\Delta^{17}O$ of OH and H_2O are zero. The estimated NO_2 $\Delta^{17}O$ values for fall-winter (34-45 ‰ daytime, 25-36 ‰ nighttime) and summer sets (25-34 ‰ for daytime; 15-24 ‰ for nighttime) represent the extremes assuming daytime oxidation takes place 100 % through the OH pathway and nighttime oxidation takes place entirely through the N_2O_5 pathway. One should keep in mind that the Alberta results are for nitrates collected during multi-week sampling periods. Each nitrate sample therefore contains *a priori* a mixture of O from the pathways operating during daytime (R6) and nighttime (R4-R7-R8). Assuming a 50 % contribution from each pathway for summer, we generate values ranging from 20 to 29 ‰. Alternatively, assuming the domination of the N_2O_5 pathway during winter (90 %; Michalski et al., 2014), the range shrinks to 26-37 ‰. Fall and spring values should fit between these summer and winter estimated ranges.

The estimated NO_2 $\Delta^{17}O$ ranges indicate that the potential parent NO_2 generally had a smaller ^{17}O anomaly than O_3 (39 ‰; Vicars and Savarino, 2014) or NO_2 in isotopic equilibrium with O_3 alone (45 ‰; Michalski et al., 2014). Two mechanisms could be responsible for the difference with the latter. One is the competition of R3 with R2 in oxidizing NO to NO_2, since RO_2 will dilute the $\Delta^{17}O$ relative to an ozone-only equilibrium. The relative reaction rates of R2 and R3 have previously been assumed to control the NO_2 isotopic composition (e.g., Alexander et al., 2009) based on the assumption of isotopic steady state. A larger contribution of RO_2 is expected in the NO_2 precursors for summer relative to winter, since biogenic VOCs that are major sources of RO_2 radicals are much higher in the summer. This suggestion is consistent with the lower $\Delta^{17}O$ ranges in summer reported here. A second possibility is that the NO_2 did not reach isotopic steady state with O_3 and RO_2, retaining some of its original signature (assumed to be $\Delta^{17}O=0$). Most studies have assumed that since photochemical steady state is established within a few minutes after emission of NO_x from a combustion source, isotopic steady state is also reached quickly. However, recent modeling by Michalski et al. (2014) suggests that isotopic equilibration of NO_x with O_3 could take up to a few hours at the relatively low NO_x and O_3 concentrations in rural Alberta. At the measured average wind speeds on site of 8-19 km hr^{-1}, transit times could be 9 minutes to almost 4 hours. Therefore, the nitrates measured at our sites may partly derive from NOx

Atmos. Chem. Phys. Discuss., https://doi.org/10.5194/acp-2017-1103
Manuscript under review for journal Atmos. Chem. Phys.
Discussion started: 9 January 2018

Atmospheric Chemistry and Physics Discussions

that had not yet reached isotopic steady state with O_3 (and RO_2). The extent of the $\Delta^{17}O$ difference between the summer and fall-winter HNO_3 clusters (Fig. 2B) likely reflects various combinations of these two mechanisms.

A challenging question is why do the HNO_3 to p-NO_3^- isotopic differences shift seasonally (Figs. 3, 4)? One factor that may influence the relationship between HNO_3 and p-NO_3^- is mass-dependent isotopic equilibrium between NH_4NO_3 and HNO_3 (R4, R7-R8 and R9-R10); however, this mechanism would result in higher $\delta^{18}O$ in p-NO_3^- and unchanged $\Delta^{17}O$ values and, therefore, cannot be solely responsible for any of the observed patterns (Fig. 3). Alternately, the trend for cold months (trend *i*) could be due to the fact that the heterogeneous N_2O_5 pathway is likely to contribute more to p-NO_3^- than to HNO_3(g), which would result in a higher contribution from ozone and explain why $\delta^{18}O$ and $\Delta^{17}O$ values are both higher in p-NO_3^-. A previous study addressing why p-NO_3^- on coarse particles is more enriched than on fine particles invoked a similar explanation (Patris et al., 2007).

For some of the spring and summer samples, both $\delta^{18}O$ and $\Delta^{17}O$ were lower in p-NO_3^- than in HNO_3 (trend *iv*), therefore the mechanism above cannot dominate the fractionation; nor can a mass-dependent process be responsible. We suggest a different fractionation process because HNO_3 dry deposits to surfaces more rapidly than p-NO_3^- (Zhang et al., 2009; Benedict et al., 2013), which would only apply in the situation where NO_2 is not in isotopic equilibrium with O_3 in a fresh plume. The first nitrates formed in the plume shortly after emission from the NO_x source have low $\delta^{18}O$ and $\Delta^{17}O$ values since NO_x has not yet reached isotopic steady state with O_3 and RO_2. Those nitrates that form as p-NO_3^- or that partition to p-NO_3^- remain in the plume for longer than HNO_3, which deposits more rapidly upon contact with vegetation or other surfaces. As the plume travels, the NO_x becomes more enriched, and the newly formed nitrates take on higher $\delta^{18}O$ and $\Delta^{17}O$ values. However, p-NO_3^- collected downwind will be a mixture of the low-$\delta^{18}O$ and -$\Delta^{17}O$ nitrate formed earlier and the high-$\delta^{18}O$ and -$\Delta^{17}O$ nitrate formed more recently, while HNO_3 will have less of the low- $\delta^{18}O$ and -$\Delta^{17}O$ nitrate. The fact that we find the lowest values in summer p-NO_3^- samples collected from various industries at distance less than 16 km supports this suggestion (Table 1). Seasonal changes in the planetary boundary layer height may also affect the impingement of emission plumes on the measurement sites, and thereby the relative amounts of fresh vs background nitrates.

The two mechanisms that we have proposed – differential N_2O_5 contribution resulting in higher $\Delta^{17}O$ values in p-NO_3^- than in HNO_3, and differential deposition resulting in lower $\Delta^{17}O$ values in p-NO_3 – would essentially compete against each other, with local conditions and chemistry influencing the results. In winter, when the N_2O_5 pathway is most important, the first mechanism dominates, as supported by the observation that p-NO_3^- concentrations are higher during that season. Conversely, in summer, when the N_2O_5 pathway is less important and dry deposition is likely faster due to minimal snow cover, higher surface wetness and high leaf areas, the second mechanism is more important. The local reactant concentrations, wind speeds and radiative fluxes (which control the time to reach isotopic equilibrium) would also be factors in the second mechanism. Therefore, we would expect intermediate trends (*ii, iii*) in other seasons. In addition to these non-mass-dependent fractionation processes, mass-dependent fractionation in formation and loss of nitrate likely contributes to the observed $\delta^{18}O$ differences. For instance, kinetic fractionation may be involved in the production of trend *iii*.

Atmos. Chem. Phys. Discuss., https://doi.org/10.5194/acp-2017-1103
Manuscript under review for journal Atmos. Chem. Phys.
Discussion started: 9 January 2018

Atmospheric Chemistry and Physics Discussions

In summary, the $\delta^{18}O$ and $\Delta^{17}O$ patterns of the measured nitrates follow the generally described seasonal isotopic trend from high, during cold periods, to low, during warm periods. However, examining the isotopic relationship of HNO_3 to p-NO_3^- (Fig. 3), and by extension w-NO_3^-, reveals the complexity of anthropogenic NOx oxidation mechanisms. The final isotopic values are derived from the O_3-NO_x (Leighton) cycle - –possibly not yet at isotopic steady state - followed by the OH and N_2O_5 (O_3) oxidation pathways in proportions that vary with the periods of sampling (Fig. 4). The negative isotopic difference between p-NO_3^- and HNO_3 during warm months likely reflects differential removal rates from plumes containing NO_x at disequilibrium with O_3. The isotopic signals from NO_x to the final nitrate species follow the isotopic trajectory of the dominant reactions, so we conceive the final oxidation trends as lines resulting from adding vectors that represent these main trajectories (Fig. 4).

4.2 Correlations with other meteorological parameters and co-pollutants

The distribution and proportion of HNO_3 and p-NO_3^- in polluted air masses can vary daily and seasonally with temperature, relative humidity (RH) and concentration of co-contaminants (Morino et al., 2006). For that reason, we compared the isotopic ratios of the HNO_3 and p-NO_3 samples with meteorological and air quality parameters measured routinely at nearby monitoring stations where available (within 5 km). We found that the p-NO_3^- and HNO_3 $\delta^{18}O$ and $\Delta^{17}O$ values correlate with RH, with p-NO_3 values showing stronger statistical links than HNO_3 (Table 6). The N_2O_5 hydrolysis reaction (R8) rate increases with humidity (Kane et al., 2001), which may explain this positive correlation. Significant inverse relationships exist between temperature and p-NO_3^- $\delta^{18}O$, p-NO_3^- $\Delta^{17}O$, and HNO_3 $\Delta^{17}O$. These negative links likely arise since N_2O_5 is more stable under cold conditions, leading to a higher contribution of R8. The stronger links with p-NO_3^- may be due to R8 taking place on surfaces (such as particles) with liquid water, which is likely to retain the HNO_3 as p-NO_3^- rather than release it to the gas phase. Therefore, in winter R8 may contribute more to p-NO_3 than to HNO_3(g), supporting our interpretation of trend *i* (Fig. 4). Moreover, the highest $\delta^{18}O$ and $\Delta^{17}O$ values were found for fall-winter samples with proportions of 33 to 66 % for HNO_3 and p-NO_3^-, respectively, and collected at high RH (76 %) and low temperature (-10°C). In contrast, the lowest p-NO_3^- isotopic values were found for samples with similar proportions of HNO_3 and p-NO_3^-, and sampled during moderately humid (60-63 %) and warm (8-20°C) periods. In other words, the HNO_3 and p-NO_3^- results obtained here partly support the previous suggestion that temperature and RH amounts can shift nitrate partitioning between HNO_3 and p-NO_3^- (Morino et al., 2006).

Concentrations of oxidants, co-contaminants (e.g., SO_4^- aerosols) and NO_x influence the dominance and rates of the discussed reactions (Brown et al., 2006; Michalski et al., 2014). For instance, high NOx/O_3 ratios do not favor NO oxidation by peroxy radicals (RO_2 family) with typically low isotopic values, explaining the positive link between $\delta^{18}O$ and $\Delta^{17}O$ values with NOx/O_3 ratios (Table 6). It appears however that the PM and SO_2 concentrations were not correlated with the production of the measured nitrates. Surprisingly, only the p-NO_3^- $\Delta^{17}O$ and $\delta^{18}O$ values correlated with the fraction of each sample collected during daylight hours (i.e., between the sunrise and sunset times on the day at the middle of each sampling period, either at Edmonton or Lethbridge), which was expected for HNO_3 as well due to the daytime-only OH pathway. However, daylight hours do not take into account light intensity, which can influence significantly the oxidation rate through this pathway, and consequently both the $\delta^{18}O$ and $\Delta^{17}O$ values.

Atmos. Chem. Phys. Discuss., https://doi.org/10.5194/acp-2017-1103
Manuscript under review for journal Atmos. Chem. Phys.
Discussion started: 9 January 2018

Atmospheric Chemistry and Physics Discussions

4.3 - $\delta^{18}O$ and $\Delta^{17}O$ in w- and p-NO_3^- from polluted areas

Atmospheric nitrates measured in central and southern Alberta were sampled downwind of well-identified anthropogenic sources to verify the potential role of emitted NO_x isotopic signals through to final nitrate isotopic ratios (primarily N isotopes; see Savard et al., 2017). As expected, the measured oxygen isotopes of the various nitrate groups show no source-specific isotopic characteristics, but instead are consistent with exchange with O_3 and oxidation through the well-known OH and N_2O_5 oxidation paths. However, NO_2 not in isotopic equilibrium with O_3, and/or NO reacted with RO_2 significantly influenced the overall results. Co-contaminants in the emissions and sampled plumes at short distances from the sources may have favoured these two mechanisms, and quantifying RO_2 and/or HO_2 would help distinguish between the two mechanisms. The question remains: are these overall effects observable in triple oxygen isotopes of nitrates from other polluted sites?

The full $\Delta^{17}O$ and $\delta^{18}O$ ranges for p-NO_3^-, w-NO_3^- and HNO_3 (between 13.8 and 20.5 ‰, 48.4 and 83.2 ‰; Table 4) compare well with the isotopic ranges obtained for bulk deposition NO_3^- samples collected downwind from oil sands mining operations in the lower Athabasca region farther north in Alberta (Proemse et al., 2013). Moreover, the isotopic clusters in cold and warm months delineated here essentially overlap with the data sets of winter and summer from the lower Athabasca region (Fig. 5). This correspondence exists despite the slightly different climatic conditions (SI-Fig. 1), different source types, and very different sampling methods (bulk/throughfall deposition samples using open ion exchange resin collectors, vs. wind sector-specific active sampling on filters and precipitation-only collectors). Notably, many points carry relatively low $\delta^{18}O$ and $\Delta^{17}O$ values.

Previous work in the Athabasca region reported very low $\delta^{18}O$ and near-zero $\Delta^{17}O$ values for p-NO_3^- sampled directly within oil-sands industrial stacks, i.e., in the emissions measured in-stack and diluted with ambient air (Proemse et al., 2012). These values appear near the O_2-end of the O_2-O_3-NO_x line (Fig. 4). Similar isotopic signatures are very likely produced in source emissions of NO_x in the studied Edmonton and Vauxhall areas (e.g., CFPP, gas compressors, industries). This source signature may persist into p-NO_3 collected close to the sources. Within the first few hours in the atmosphere (or less, in more polluted areas), the NO_x $\delta^{18}O$ and $\Delta^{17}O$ values rapidly increase due to isotope exchange with O_3 via many iterations of the photochemical NO_x-O_2-O_3 cycle (R2, R3, R5 and O3 formation, Table 5; Michalski et al., 2014) and reach isotopic equilibrium. Though the e-folding lifetime for NO_x oxidation to nitrates may be longer than these few hours, depending on the NO_x/VOC ratio, only a fraction of the oxidized source NO_x will create a measureable contribution to the ambient nitrate where the background air is very low in nitrate. This is likely the case in the oil sands region, where Proemse et al. (2013) reported the lowest $\Delta^{17}O$ values within 12 km of the emission sites, and where direct stack emissions of p-NO_3^- were ~5000 times lower than NO_x emissions (Wang et al., 2012).

In a methodological test study, we obtained low values for w-NO_3^- sampled near a high traffic volume highway in Ontario, Canada (Smirnoff et al., 2012). Low $\delta^{18}O$ and $\Delta^{17}O$ values in atmospheric nitrates during warm months (65 and 20 ‰ or less, respectively) have been reported for other parts of the world as well (Table 4). Authors of these studies have invoked peroxy radicals to account for low $\delta^{18}O$ values in w-NO_3^- from a polluted city (Fang et al., 2011), in p-NO_3^- from Taiwan collected partly from air masses influenced by pollutants (Guha et al., 2017) and from a polluted coastal site in California (Michalski et

al., 2004; Patris et al., 2007; Table 4). However, sampling in these three other regions did not use collection restricted to air masses transported from targeted anthropogenic sources. So uncertainties persist regarding the ultimate sources of nitrates with low isotopic values.

Although a few low values are also reported for seemingly non-polluted areas of the Arctic and Antarctic regions (unknown cause; Morin et al., 2008; Morin et al., 2009), and of coastal California (Patris et al., 2007), the information from the literature, integrated with the interpretation proposed for the Alberta low $\delta^{18}O$ and $\Delta^{17}O$ values in summer nitrates, may reflect the involvement of air masses that favour RO_2 reactions and/or include nitrates from oxidation of NO_x with light isotopes in plumes. In such cases, we hypothesize that the NO_x-O_3 isotopic equilibrium was not reached (see Section 4.1). Keeping in mind that other hydrocarbon and halogen pathways may play a role in determining the isotopic nitrate characteristics in other parts of the world, we propose that, in general, the warm-periods isotopic ranges appear to be lower in polluted areas, regardless of the anthropogenic source types. Given these points, our nitrate $\delta^{18}O$ and $\Delta^{17}O$ values do not represent indicators of specific sources but, more likely, in the case of summer solid phases, they may reflect anthropogenic nitrates in general. Further research work on plume NO_x to nitrates chemical mechanisms may help to validate this suggestion.

4.4 Comparison with high-latitude p-NO_3^-

An interesting aspect of the Alberta p-NO_3^- cold-period $\Delta^{17}O$ ranges is that they compare relatively well with the range obtained for Canadian Arctic winter (Fig. 6), during which nighttime conditions and the N_2O_5 pathway prevail without interruption (Morin et al., 2008). This observation supports the suggestion that the N_2O_5 pathway produces around 90 % of nitrates during mid-latitudinal cold months (Michalski et al., 2003; Section 4.1). The $\delta^{18}O$ ranges of cold months are similar in Alberta and in the Arctic. This similarity goes against previous suggestions that at higher latitudes, nitrate $\delta^{18}O$ annual means should be higher than at mid-latitudes due to local ambient conditions and atmospheric chemistry affecting the proportions of species involved in producing nitrate (Morin et al., 2009), namely, the sole influence of the N_2O_5 pathway during the Arctic winter (Fang et al., 2011).

The $\Delta^{17}O$ departure between the Alberta and Arctic winter parallel lines is about 3‰. Such difference is slightly larger than the one calculated for winter NO_3^- at 80 and 40° N latitudes (about 2 ‰; Morin et al., 2008). In contrast, the warm-months and summer data sets for Alberta and the Arctic, respectively, show different isotopic ranges (Fig. SI-3), possibly due to the plume effects described in Section 4.3. Moreover, contrary to a previous suggestion, the winter-summer contrast in nitrate $\Delta^{17}O$ values is similar at the mid- and high-latitudinal sites (about 6 ‰ here, and 5 ‰ in Morin et al., 2008). This similarity is likely coincidental as it may reflect the fact that during warm months the anthropogenic influence may lower the summer $\Delta^{17}O$ values in Alberta (see Section 4.1), whereas the seasonal departure in Arctic samples comes from the dominant OH and N_2O_5 pathways during summer and winter, respectively. Finally, the $\Delta^{17}O$ averages for the Alberta summer and winter results approximately fits within ranges predicted for the studied area by global modeling (Alexander et al., 2009), suggesting that global modeling of nitrate distribution worldwide is promising. In the future, the assumption of NO_x isotopic steady state with O_3 should be explored, given recent findings (Michalski et al., 2014), the critical importance of NO_x isotope characteristics on resulting

nitrate isotopic values (Alexander et al., 2009), and the suggestion regarding the evolution of NO_x-NO_3^- signals in early anthropogenic plumes (present study).

5 Conclusion

The HNO_3, w-NO_3 and p-NO_3 from five different sources in central and southern Alberta, simultaneously collected with wind sector-based conditional sampling systems produced similar $\delta^{18}O$ and $\Delta^{17}O$ trends, regardless of their sources types (CFPP, various industries, city traffic, and gas compressors). This confirms previous observations that regional ambient conditions (e.g., light intensity, RH, temperature) dictate the triple isotopic characteristics and oxidation pathways of nitrates.

The gaseous form of nitrate (HNO_3) having distinct isotopic characteristics relative to the wet and particulate forms imply that understanding nitrate formation and loss requires characterizing the nitrate species individually, and disavows the assumption that isotopic values of the nitrate phases are invariably interchangeable. The Albertan nitrate production operated mostly through the well-known OH and N_2O_5 oxidation pathways, possibly prior to their reaching isotopic equilibrium with O_3 in some samples, though we also suggest contributions from RO_2 oxidation of NO, as well leading to low oxygen isotopic values. Particulate-NO_3^- generally shows higher $\delta^{18}O$ and $\Delta^{17}O$ values than HNO_3 in the fall-winter period as the heterogeneous N_2O_5 pathway favours the production of p-NO_3^-. Moreover, HNO_3 has higher $\delta^{18}O$ and $\Delta^{17}O$ values during warm periods, which we propose is due to faster dry deposition rates relative to p-NO_3^- in the event that NO_x is oxidized before reaching isotopic steady state with O_3. These mechanisms conferring p-NO_3^- with relatively low isotopic values are prone to happen in anthropogenic polluted air masses. An interesting deduction arising from this interpretation and from a comparison with nitrate isotopes from other polluted areas of the world is that relatively low $\delta^{18}O$ and $\Delta^{17}O$ values may reflect nitrates produced from undifferentiated anthropogenic NO_x emissions.

Future research needs to explore the assumption of NO_x isotopic equilibration with O_3, given the critical importance of NO_x isotopes on resulting nitrate isotopic values. More field sampling and state-of-the-art isotopic analyses of all tropospheric nitrate species, as well as NO_x, are required for refining our understanding of atmospheric nitrate worldwide. This endeavour is fundamental for developing effective emission-reduction strategies towards improving future air quality.

Acknowledgements. The authors are grateful for the technical support provided by Marie-Christine Simard and Jade Bergeron of the Geological Survey of Canada, and by Syed Iqbal, Rachel Mintz, Daniel McLennan, Matthew Parsons, Mike Shaw Amy Hou of Environment and Climate Change Canada; and for the constructive pre-submission review by Drs. Geneviève Bordeleau from the Geological Survey of Canada, and Felix Vogel and Jason O'Brien from ECCC. This research has been financially supported by the Clean Air Regulatory Agenda of Environment and Climate Change Canada, and the Environmental Geoscience program of Natural Resources Canada (NRCan contribution number: 20170310). The first author dedicates this research article to Pauline Durand for her support.

Atmos. Chem. Phys. Discuss., https://doi.org/10.5194/acp-2017-1103
Manuscript under review for journal Atmos. Chem. Phys.
Discussion started: 9 January 2018

Atmospheric Chemistry and Physics Discussions

References

Alexander, B., Hastings, M. G., Allman, D. J., Dachs, J., Thornton, J. A., and Kunasek, S. A.: Quantifying atmospheric nitrate formation pathways based on a global model of the oxygen isotopic composition (δ17O) of atmospheric nitrate, Atmospheric Chemistry and Physics, 9, 5043-5056, 2009.

Benedict, K. B., Carrico, C. M., Kreidenweis, S. M., Schichtel, B., Malm, W. C., and Collett Jr, J. L.: A seasonal nitrogen deposition budget for Rocky Mountain National Park, Ecological Applications, 23, 1156-1169, 10.1890/12-1624.1, 2013.

Brown, S. S., Ryerson, T. B., Wollny, A. G., Brock, C. A., Peltier, R., Sullivan, A. P., Weber, R. J., Dubé, W. P., Trainer, M., Meagher, J. F., Fehsenfeld, F. C., and Ravishankara, A. R.: Variability in nocturnal nitrogen oxide processing and its role in regional air quality, Science, 311, 67-70, 10.1126/science.1120120, 2006.

Cheng, I., and Zhang, L.: Long-term air concentrations, wet deposition, and scavenging ratios of inorganic ions, HNO3, and SO2 and assessment of aerosol and precipitation acidity at Canadian rural locations, Atmospheric Chemistry and Physics, 17, 4711-4730, 10.5194/acp-17-4711-2017, 2017.

Clark, I., and Fritz, P.: Environmental Isotopes in Hydrogeology Lewis, 1997.

Coplen, T. B., Böhlke, J. K., and Casciotti, K.: Rapid Commun. Mass Spectrom., 18, 245, 2004.

Dahal, B., and Hastings, M. G.: Technical considerations for the use of passive samplers to quantify the isotopic composition of NO x and NO 2 using the denitrifier method, Atmospheric Environment, 143, 60-66, 2016.

Dubey, M. K., Mohrschladt, R., Donahue, N. M., and Anderson, J. G.: Isotope specific kinetics of hydroxyl radical (OH) with water (H2O): Testing models of reactivity and atmospheric fractionation, Journal of Physical Chemistry A, 101, 1494-1500, 1997.

Elliott, E. M., Kendall, C., Boyer, E. W., Burns, D. A., Lear, G. G., Golden, H. E., Harlin, K., Bytnerowicz, A., Butler, T. J., and Glatz, R.: Dual nitrate isotopes in dry deposition: Utility for partitioning NO x source contributions to landscape nitrogen deposition, Journal of Geophysical Research: Biogeosciences, 114, 10.1029/2008JG000889, 2009.

Environment and Climate Change Canada; Air Pollutant Emission Inventory Online Data Query: http://www.ec.gc.ca/inrp-npri/donnees-data/ap/index.cfm?lang=En, access: accessed 2016/12/15, 2016.

Erisman, J. W., and Fowler, D.: Oxidized and reduced nitrogen in the atmosphere, Knowledge for Sustainable Development, An Insight into the Encyclopedia of Life Support Systems, Volumes I, II, III, UNESCO Publishing-Eolss Publishers, Oxford, UK, 2003.

Fang, Y. T., Koba, K., Wang, X. M., Wen, D. Z., Li, J., Takebayashi, Y., Liu, X. Y., and Yoh, M.: Anthropogenic imprints on nitrogen and oxygen isotopic composition of precipitation nitrate in a nitrogen-polluted city in southern China, Atmospheric Chemistry and Physics, 11, 1313-1325, 10.5194/acp-11-1313-2011, 2011.

Guha, T., Lin, C. T., Bhattacharya, S. K., Mahajan, A. S., Ou-Yang, C. F., Lan, Y. P., Hsu, S. C., and Liang, M. C.: Isotopic ratios of nitrate in aerosol samples from Mt. Lulin, a high-altitude station in Central Taiwan, Atmospheric Environment, 154, 53-69, 10.1016/j.atmosenv.2017.01.036, 2017.

Hastings, M. G., Sigman, D. M., and Lipschultz, F.: Isotopic evidence for source changes of nitrate in rain at Bermuda, Journal of Geophysical Research D: Atmospheres, 108, ACH 22-21 - ACH 22-12, 2003.

IPCC; Fifth Assessment Report (AR5): https://www.ipcc.ch/report/ar5/, access: September 2017, 2013.

Johnston, J. C., and Thiemens, M. H.: The isotopic composition of tropospheric ozone in three environments, Journal of Geophysical Research Atmospheres, 102, 25395-25404, 1997.

Kaiser, J., Hastings, M. G., Houlton, B. Z., Röckmann, T., and Sigman, D. M.: Triple oxygen isotope analysis of nitrate using the denitrifier method and thermal decomposition of N2O, Analytical Chemistry, 79, 599-607, 10.1021/ac061022s, 2007.

Kane, S. M., Caloz, F., and Leu, M. T.: Heterogeneous uptake of gaseous N2O5 by (NH4)2SO4, NH4HSO4, and H2SO4 aerosols, Journal of Physical Chemistry A, 105, 6465-6470, 10.1021/jp010490x, 2001.

Kendall, C., Elliott, E. M., and Wankel, S. D.: Tracing Anthropogenic Inputs of Nitrogen to Ecosystems, in: Stable Isotopes in Ecology and Environmental Science: Second Edition, 375-449, 2007.

Lavoie, G. A., Heywood, J. B., and Keck, J. C.: EXPERIMENTAL AND THEORETICAL STUDY OF NITRIC OXIDE FORMATION IN INTERNAL COMBUSTION ENGINES, M, I.T.-Dept Mech Eng-Fluid Mechanics Laboratory Publ 69-10, 1969.

Liang, M. C., and Yung, Y. L.: Sources of the oxygen isotopic anomaly in atmospheric N<inf>2</inf>O, Journal of Geophysical Research Atmospheres, 112, 10.1029/2006JD007876, 2007.

Michalski, G., Scott, Z., Kabiling, M., and Thiemens, M. H.: First measurements and modeling of Δ17O in atmospheric nitrate, Geophysical Research Letters, 30, 14-11, 2003.

Michalski, G., Meixner, T., Fenn, M., Hernandez, L., Sirulnik, A., Allen, E., and Thiemens, M.: Tracing Atmospheric Nitrate Deposition in a Complex Semiarid Ecosystem Using Δ17O, Environmental Science and Technology, 38, 2175-2181, 10.1021/es034980+, 2004.

Michalski, G., Bhattacharya, S. K., and Girsch, G.: NOx cycle and the tropospheric ozone isotope anomaly: An experimental investigation, Atmospheric Chemistry and Physics, 14, 4935-4953, 10.5194/acp-14-4935-2014, 2014.

Morin, S., Savarino, J., Bekki, S., Gong, S., and Bottenheim, J. W.: Signature of Arctic surface ozone depletion events in the isotope anomaly (Δ17O) of atmospheric nitrate, Atmospheric Chemistry and Physics, 7, 1451-1469, 2007.

Morin, S., Savarino, J., Frey, M. M., Yan, N., Bekki, S., Bottenheim, J. W., and Martins, J. M. F.: Tracing the origin and fate of NOx in the arctic atmosphere using stable isotopes in nitrate, Science, 322, 730-732, 10.1126/science.1161910, 2008.

Morin, S., Savarino, J., Frey, M. M., Domine, F., Jacobi, H. W., Kaleschke, L., and Martins, J. M. F.: Comprehensive isotopic composition of atmospheric nitrate in the Atlantic Ocean boundary layer from 65°S to 79°N, Journal of Geophysical Research Atmospheres, 114, 10.1029/2008JD010696, 2009.

Morin, S., Sander, R., and Savarino, J.: Simulation of the diurnal variations of the oxygen isotope anomaly (Δ17O) of reactive atmospheric species, Atmospheric Chemistry and Physics, 11, 3653-3671, 10.5194/acp-11-3653-2011, 2011.

Morino, Y., Kondo, Y., Takegawa, N., Miyazaki, Y., Kita, K., Komazaki, Y., Fukuda, M., Miyakawa, T., Moteki, N., and Worsnop, D. R.: Partitioning of HNO<inf>3</inf> and particulate nitrate over Tokyo: Effect of vertical mixing, Journal of Geophysical Research Atmospheres, 111, 10.1029/2005JD006887, 2006.

OPIC; http://wateriso.utah.edu/waterisotopes/WebCode/delta.cgi?lat=50&lon=-110.5&elev=690&Type=MonthlyInterp, 2017.

Patris, N., Cliff, S. S., Quinn, P. K., Kasem, M., and Thiemens, M. H.: Isotopic analysis of aerosol sulfate and nitrate during ITCT-2k2: Determination of different formation pathways as a function of particle size, Journal of Geophysical Research Atmospheres, 112, 10.1029/2005JD006214, 2007.

Proemse, B. C., Mayer, B., Chow, J. C., and Watson, J. G.: Isotopic characterization of nitrate, ammonium and sulfate in stack PM 2.5 emissions in the Athabasca Oil Sands Region, Alberta, Canada, Atmospheric Environment, 60, 555-563, 10.1016/j.atmosenv.2012.06.046, 2012.

Proemse, B. C., Mayer, B., Fenn, M. E., and Ross, C. S.: A multi-isotope approach for estimating industrial contributions to atmospheric nitrogen deposition in the Athabasca oil sands region in Alberta, Canada, Environmental Pollution, 182, 80-91, 10.1016/j.envpol.2013.07.004, 2013.

Randles, R. H., and Wolfe, D. A.: Introduction to the theory of nonparametric statistics, Wiley New York, 1979.

Röckmann, T., Brenninkmeijer, C. A. M., Saueressig, G., Bergamaschi, P., Crowley, J. N., Fischer, H., and Crutzen, P. J.: Mass-independent oxygen isotope fractionation in atmospheric CO as a result of the reaction CO + OH, Science, 281, 544-546, 10.1126/science.281.5376.544, 1998.

Rolph, G. D.; Real-time Environmental Applications and Display sYstem (READY): http://www.ready.noaa.gov, access: January, 2017.

Savard, M. M., Cole, A., Smirnoff, A., and Vet, R.: δ15N values of atmospheric N species simultaneously collected using sector-based samplers distant from sources – Isotopic inheritance and fractionation, Atmospheric Environment, 162, 11-22, 10.1016/j.atmosenv.2017.05.010, 2017.

Savarino, J., Kaiser, J., Morin, S., Sigman, D. M., and Thiemens, M. H.: Nitrogen and oxygen isotopic constraints on the origin of atmospheric nitrate in coastal Antarctica, Atmospheric Chemistry and Physics, 7, 1925-1945, 2007.

Savarino, J., Bhattacharya, S. K., Morin, S., Baroni, M., and Doussin, J. F.: The NO+ O3 reaction: A triple oxygen isotope perspective on the reaction dynamics and atmospheric implications for the transfer of the ozone isotope anomaly, Journal of Chemical Physics, 128, 10.1063/1.2917581, 2008.

Sirois, A., and Vet, R.: The Precision of Precipitation Chemistry Measurements in the Canadian Air and Precipitation Monitoring Network (CAPMoN), Environmental Monitoring and Assessment, 57, 301-329, 10.1023/a:1006035129393, 1999.

Smirnoff, A., Savard, M. M., Vet, R., and Simard, M. C.: Nitrogen and triple oxygen isotopes in near-road air samples using chemical conversion and thermal decomposition, Rapid Communications in Mass Spectrometry, 26, 2791-2804, 10.1002/rcm.6406, 2012.

Stein, A., Draxler, R., Rolph, G., Stunder, B., Cohen, M., and Ngan, F.: NOAA's HYSPLIT atmospheric transport and dispersion modeling system, Bulletin of the American Meteorological Society, 96, 2059-2077, 2015.

Stroud, C. A., Jonathan; Leiming, Zhang; Flagg, David; Makar, Paul: Atmospheric processes, Chapitre 2 - Draft version, in, Canadian smow Science Assessment, 2008.

Thiemens, M. H.: Mass-independent isotope effects in planetary atmospheres and the early solar system, Science, 283, 341-345, 10.1126/science.283.5400.341, 1999.

Tsunogai, U., Komatsu, D. D., Daita, S., Kazemi, G. A., Nakagawa, F., Noguchi, I., and Zhang, J.: Tracing the fate of atmospheric nitrate deposited onto a forest ecosystem in Eastern Asia using Δ17O, Atmospheric Chemistry and Physics, 10, 1809-1820, 2010.

Vicars, W. C., Bhattacharya, S. K., Erbland, J., and Savarino, J.: Measurement of the 17O-excess (δ 17O) of tropospheric ozone using a nitrite-coated filter, Rapid Communications in Mass Spectrometry, 26, 1219-1231, 10.1002/rcm.6218, 2012.

Vicars, W. C., Morin, S., Savarino, J., Wagner, N. L., Erbland, J., Vince, E., Martins, J. M. F., Lerner, B. M., Quinn, P. K., Coffman, D. J., Williams, E. J., and Brown, S. S.: Spatial and diurnal variability in reactive nitrogen oxide chemistry as reflected in the isotopic composition of atmospheric nitrate: Results from the CalNex 2010 field study, Journal of Geophysical Research Atmospheres, 118, 10567-10588, 10.1002/jgrd.50680, 2013.

Vicars, W. C., and Savarino, J.: Quantitative constraints on the 17O-excess (δ17O) signature of surface ozone: Ambient measurements from 50°N to 50°S using the nitrite-coated filter technique, Geochimica et Cosmochimica Acta, 135, 270-287, 10.1016/j.gca.2014.03.023, 2014.

Walters, W. W., and Michalski, G.: Theoretical calculation of oxygen equilibrium isotope fractionation factors involving various NOy molecules, OH, and H 2 O and its implications for isotope variations in atmospheric nitrate, Geochimica et Cosmochimica Acta, 191, 89-101, 2016.

Wang, X. L., Watson, J. G., Chow, J. C., Kohl, S. D., Chen, L. W. A., Sodeman, D. A., Legge, A. H., and Percy, K. E.: Measurement of Real-World Stack Emissions with a Dilution Sampling System, in: Developments in Environmental Science, 171-192, 2012.

Zel'dovich, Y. B.: The Oxidation of Nitrogen in Combustion and Explosions, Acta Physicochimica, 21, 577-628, 1946.

Zhang, L., Vet, R., O'Brien, J. M., Mihele, C., Liang, Z., and Wiebe, A.: Dry deposition of individual nitrogen species at eight Canadian rural sites, Journal of Geophysical Research Atmospheres, 114, 10.1029/2008JD010640, 2009.

Atmos. Chem. Phys. Discuss., https://doi.org/10.5194/acp-2017-1103
Manuscript under review for journal Atmos. Chem. Phys.
Discussion started: 9 January 2018

Atmospheric Chemistry and Physics Discussions

Table 1. Settings and conditions for wind sector-based simultaneous sampling of atmospheric nitrates.

Site (coordinates)	**Sources**	**Distance** Km (mean)	**Sector** direction; opening	**Sampling** period;	**n**	**Avg T** (°C)	**Context**
Genesee (114.14° W, 53.31° N)	Coal-fired power plants	7–25	NW, 35°	30/09/2010 – 21/06/2011	6	11.7, 12.2, 5.5, -9.8, -0.9, 12.2	3 plants
Vauxhall (112.11° W, 50.06° N)	Gas compressors and cattle and swine feedlots	12-125+; 7.5-45+	W, 65°	25/10/2011 – 13/12/2011	3	2.6, 0.7,-3.5	65+ compressors; 200+ feedlots
Terrace Heights (113.44° W, 53.54° N)	Urban traffic	<1-15 (4)	W, 150°	24/07/2012 – 25/10/2012	4	20.3, 15.6, 7.9, -1.8	Park in residential area, 3.5 km east of downtown core
Fort Saskatchewan (113.14° W, 53.72° N)	Chemical industries and metal refining	3-7 (4)	NW, 88°	12/04/2013 – 06/09/2013	4	4.3, 15.7, 16.3, 17.7	Chemical plant and metal refinery largest NO_x sources; fertilizer plant largest NH_3 source
Fort Saskatchewan (113.14° W, 53.72° N)	Fertilizers plant and oil refinery	9-14 (11)	N, 27°	20/09/2013 – 20/01/2014	1	-8.1	Fertilizer plant largest NH_3 and NO_x source, oil refinery major NO_x source

N: number of sampling sessions. Avg T: average temperature during each of the consecutives sampling sessions.

Table 2. Isotopic reproducibility (modified median absolute deviation) established using 2 to 4 parallel active CAPMoN sampling setups in seven separate sampling periods, resulting in (n) total samples.

N compound (n)	**$\delta^{18}O$**	**$\delta^{17}O$**
Teflon filters p-NO_3^- (19)	2	1
Nylon filters HNO_3 (18)	1	0.7

Table 3. Average oxygen isotopic ratios (‰) for NO_3^- sampled as gas (HNO_3), w (precipitation) and p (particulate matter) relative to VSMOW.

Matrix	Gas	w	p	Gas	..w	..p
Source	**$\delta^{18}O$**			**$\Delta^{17}O$**		
Coal-fired power plants	69.7 (5)	66.1 (4)	70.7 (4)	25.1 (5)	25.4 (4)	26.6 (4)
Fertilizers plant & oil refinery	63.2 (1)	71.4 (1)	69.5 (1)	19.3 (1)	26.0 (1)	23.8 (1)
Chemical industries & metal refining	65.7 (4)	61.9 (2)	54.6 (4)	21.8 (4)	21.4 (2)	18.5 (4)
Gas compressors	65.0 (2)	-	63.1 (3)	24.5 (2)	-	26.4 (3)
City traffic	65.7 (3)	67.2 (2)	59.6 (3)	21.2 (3)	24.4 (2)	22.5 (3)
Mean	**66.8**	**66.0**	**62.6**	**23.0**	**24.3**	**23.4**

(n): number of sampling periods characterized

Atmos. Chem. Phys. Discuss., https://doi.org/10.5194/acp-2017-1103
Manuscript under review for journal Atmos. Chem. Phys.
Discussion started: 9 January 2018

Atmospheric Chemistry and Physics Discussions

Table 4. Compilation of triple oxygen isotopic ranges obtained for atmospheric and emitted nitrates.

$\delta^{18}O$ (‰)	$\Delta^{17}O$ (‰)	Regional context	Location	Authors
HNO_3				
62.4-81.7	19.3-29.0	Various contaminated sites	Alberta, Canada	*This study*
p-NO_3^-				
43-62	20-27	Coast, Trinidad Head	California, USA	Patris et al. (2007)
78-92	29.8-35.0	High Arctic (Alert, Ellesmere Is.)	Nunavut, Canada	Morin et al. (2007)
62-112	19-43	Coast	Antarctica	Savarino et al. (2007)
15.6-36.0	-0.2 to 1.8	Oil-sands mining stacks, PM 2.5	Alberta, Canada	Proemse et al. (2012)
49-86	19-27	Coast (onboard sampling)	California, USA	Vicars et al. (2013)
10.8-92.4	2.7-31.4	Mt. Lulin, partly polluted air masses	Central Taiwan	Guha et al. (2017)
48.4-83.2	13.8-30.5	Various contaminated sites	Alberta, Canada	*This study*
w-NO_3^-				
66.3-84.0	20.2-36.0	Shenandoah National Park	Virginia, USA	Coplen et al. (2004)
70-90	20-30	Bi-monthly sampling across state	New England, USA	Kendall et al. (2007)
68-101	20.8-34.5	Rishiri Island, polluted air masses	Northern Japan	Tsunogai et al. (2010)
51.7-72.8	18.9-28.1	Highway traffic emissions	Ontario, Canada	Smirnoff et al. (2012)
35.0-80.7	15.7-32.0	Oil-sands mining (with some dry dep)	Alberta, Canada	Proemse et al. (2013)
57.4-74.4	19.2-30.1	Various contaminated sites	Alberta, Canada	*This study*
Undifferentiated and Bulk NO_3^-				
60-95	21-29	Polluted coastal area & Remote land	California, USA	Michalski et al. (2004)
57-79	22-32	High Arctic	Nunavut, Canada	Morin et al. (2008)
36-105	13-37	Marine boundary layer	65S to 79N Atlantic	Morin et al. (2009)
56.6-82.3*	16.7-30.2*	Various contaminated sites	Alberta, Canada	*This study*

Note: isotopic values rounded at unit are from published graphs (except for O values with actual precision at unit in Morin et al., 2007).
*Calculated using weighted averages of HNO_3 and p-NO_3 isotopic results.

Table 5. Main reactions producing atmospheric nitrates (Zel'dovich, 1946; Lavoie et al., 1969; Erisman and Fowler, 2003; Michalski et al., 2003; Morino et al., 2006; Morin et al., 2007; Stroud, 2008; Michalski et al., 2014) Reactions 1, 9-12 can occur any time.

Daytime - Summer	Nighttime - Winter
(R1) $O_2 + Q \rightarrow O + O + Q$; $N_2 + O \rightarrow NO + N$; $N + O_2 \rightarrow NO + O$	
(R2) $O + O_2 + M \rightarrow O_3$; $NO + O_3 \rightarrow NO_2 + O_2$	
(R3) $NO + RO_2 \rightarrow NO_2 + RO$	
	(R4) $NO_2 + O_3 \rightarrow NO_3 + O_2$
(R5) $NO_2 + h\nu$ (sunlight) $\rightarrow NO + O$	
(R6) $NO_2 + OH + M \rightarrow HNO_3 + M$	(R7) $NO_2 + NO_3^- \Leftrightarrow N_2O_5$
	(R8) $N_2O_5 + H_2O$(surface) $\rightarrow 2HNO_3$ (aq)*
(R9) $HNO_3(g) \Leftrightarrow HNO_3(aq)^* \rightarrow NO_3^-(aq)^* + H^+(aq)$	
(R10) $HNO_3(g) + NH_3(g) \Leftrightarrow NH_4NO_3(s)$	
(R11) $HNO_3(g) + CaCO_3(s) \rightarrow Ca(NO_3)_2(s) + HCO_3$	
(R12) $NO_3^- + HC_;(CH_3)_2S \rightarrow HNO_3 + products$	

*Q is a stable molecule of high energy; M is either O_2 or N_2; RO_2 stands for both HO_2 and alkyl peroxy. HC stand for hydrocarbons. *This aqueous nitrate may be on a particle.*

Atmos. Chem. Phys. Discuss., https://doi.org/10.5194/acp-2017-1103
Manuscript under review for journal Atmos. Chem. Phys.
Discussion started: 9 January 2018

Atmospheric Chemistry and Physics Discussions

Table 6. Correlations of NO_3^- isotopic results (‰) with meteorological parameters and concentration (or ratio) of co-contaminants.

	Relative Humidity		Temperature		Daylight (fraction)		PM	SO_2	O_3		NOx/O_3	
	r	R^2	r	R^2	r	R^2	r	r	r	R^2	r	R^2
HNO_3												
$\delta^{18}O$	**0.8**	0.59	-0.4		-0.3		0.1	0.0	-0.29		0.4	0.12
n	8		15		15		13	13	13		13	
$\Delta^{17}O$	0.6		**-0.5**	0.24	-0.4		0.4	0.3	-0.03		0.2	0.06
n	8		15		15		13	13	13		13	
$p\text{-}NO_3^-$												
$\delta^{18}O$	**0.9**	0.79	**-0.6**	0.34	**-0.6**	0.35	0.1	0.5	**-0.61**	0.38	**0.6**	0.39
n	7		15		15		12	12	12		12	
$\Delta^{17}O$	**0.9**	0.73	**-0.6**	0.34	**-0.7**	0.44	0.0	0.5	-0.47		**0.7**	0.45
n	7		15		15		12	12	12		12	

In **bold** are the significant correlation coefficients, equal or above the 95 % significance value

Atmos. Chem. Phys. Discuss., https://doi.org/10.5194/acp-2017-1103
Manuscript under review for journal Atmos. Chem. Phys.
Discussion started: 9 January 2018

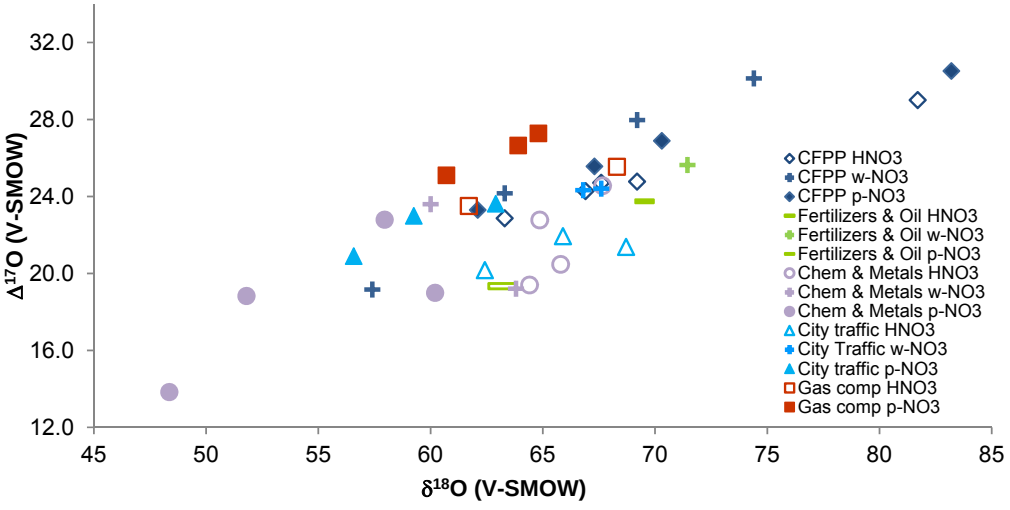

Figure 1: Triple oxygen isotopic results (‰) obtained for simultaneously sampled atmospheric HNO_3 (empty symbols), w-NO_3^- (crosses) and p-NO_3^- (full symbols) downwind of the various sources.

Atmos. Chem. Phys. Discuss., https://doi.org/10.5194/acp-2017-1103
Manuscript under review for journal Atmos. Chem. Phys.
Discussion started: 9 January 2018

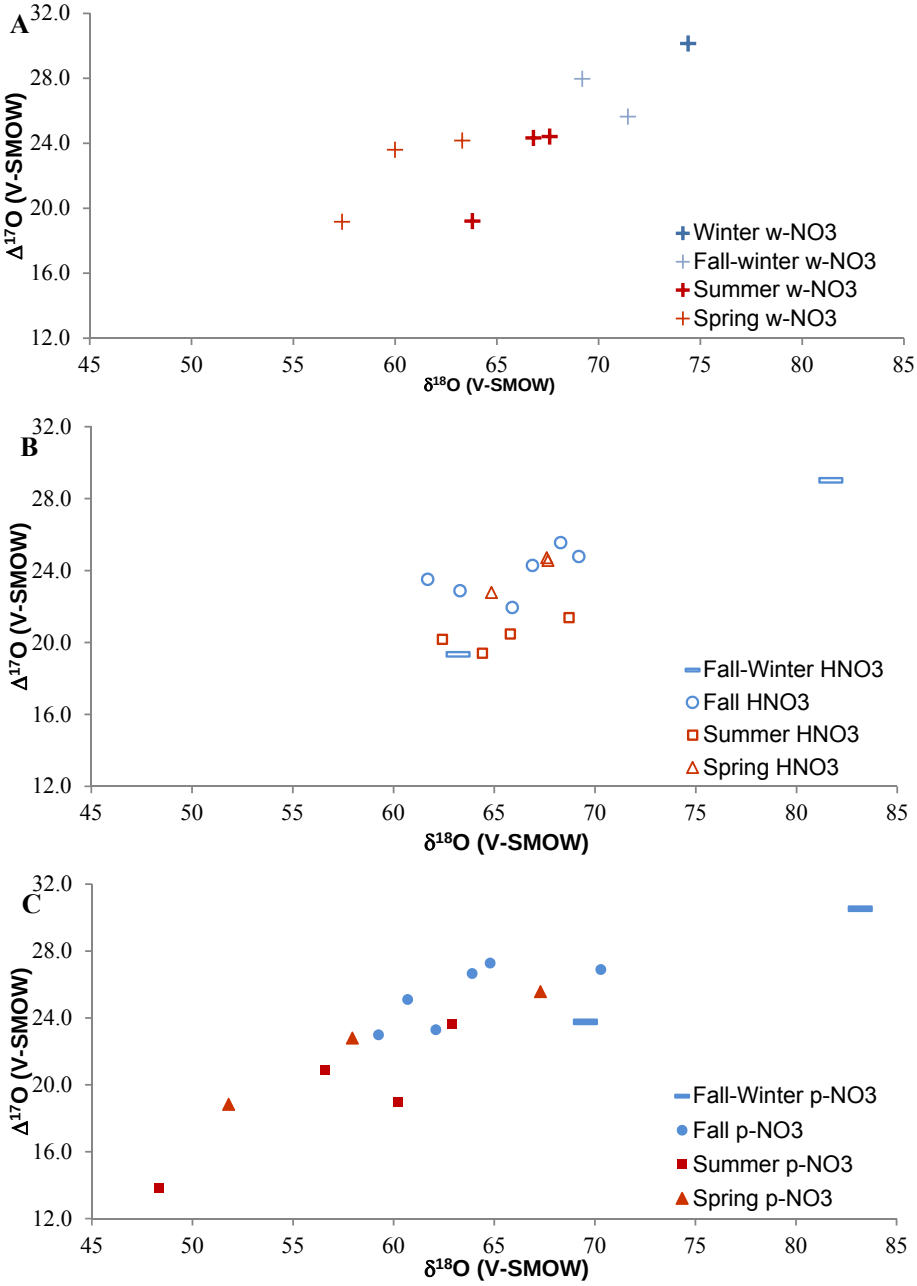

Figure 2: Triple O isotopic results (‰) obtained for simultaneously collected atmospheric HNO_3 (A), w-NO_3^- (B) and p-NO_3^- (C), in Alberta, identified by sampling periods (cold months - blue; warm months - red).

Atmos. Chem. Phys. Discuss., https://doi.org/10.5194/acp-2017-1103
Manuscript under review for journal Atmos. Chem. Phys.
Discussion started: 9 January 2018

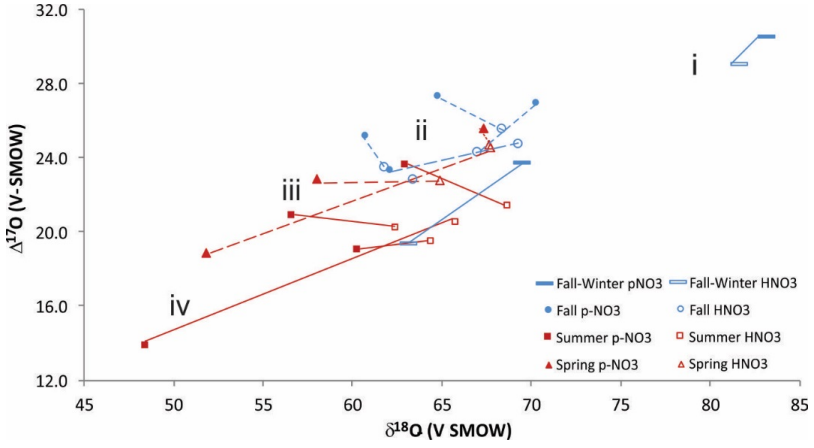

Figure 3: Line-connected $\delta^{18}O$ and $\Delta^{17}O$ values (‰) for simultaneously collected HNO_3 and p-NO_3^- from cold and warm sampling periods.

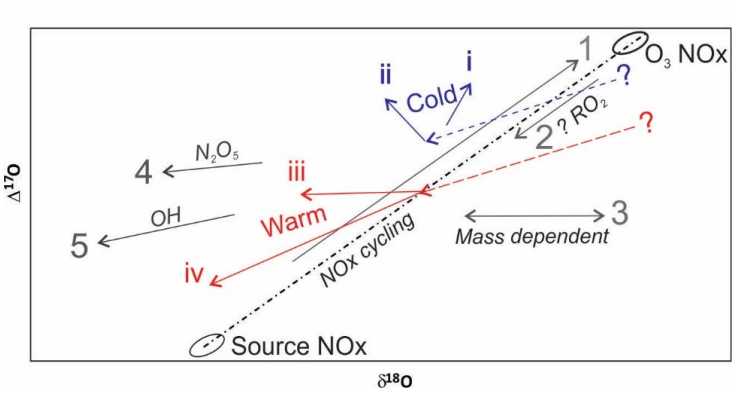

Figure 4: Schematic outline of main steps in the production of Alberta nitrates: NO_x-O_2-O_3 photochemical cycle (1) and reaction with RO_2 (2) modify NO_x source signals (R2, R3, R9); oxidation of NO_x produces HNO_3 along the N_2O_5 (4) or OH (5) pathways. The grey line represents NO_x from photochemical cycling with O_2 and O_3 (Michalski et al., 2014). The direction of arrows 1 to 5 indicates how the isotopic values would evolve along the different chemical reactions; the positions of these arrows are arbitrary.

Atmos. Chem. Phys. Discuss., https://doi.org/10.5194/acp-2017-1103
Manuscript under review for journal Atmos. Chem. Phys.
Discussion started: 9 January 2018

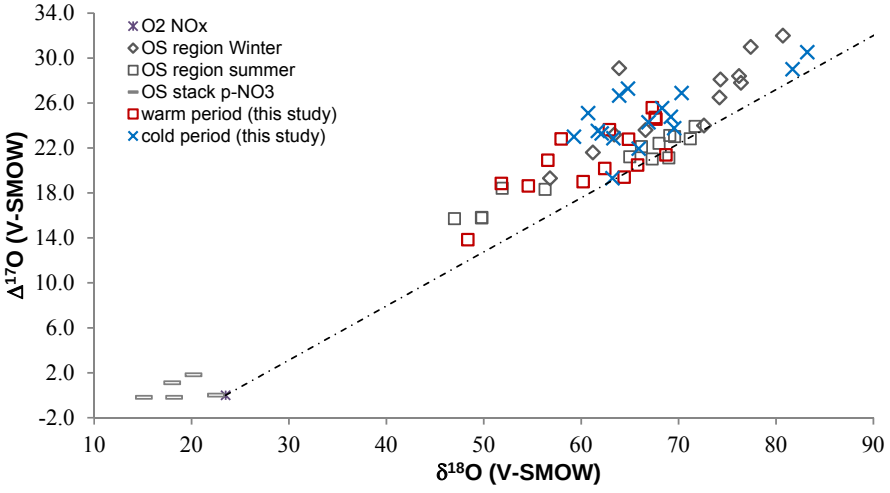

Figure 5: Isotopic ratios (‰) for atmospheric p-NO_3^-, w-NO_3^- and HNO_3 samples in cold and warm periods from central and southern Alberta (this study), compared with previously published winter and summer bulk and throughfall deposition samples from the oil sands (OS) region from northern Alberta (Proemse et al., 2013), and p-NO_3^- in-stack emissions data for an OS upgrader located in the same region (Proemse et al., 2012). The grey dotted line connects NO_x from theoretical combustion with O_2 isotopic composition and at isotopic equilibrium with tropospheric O_3 (Michalski et al., 2014).

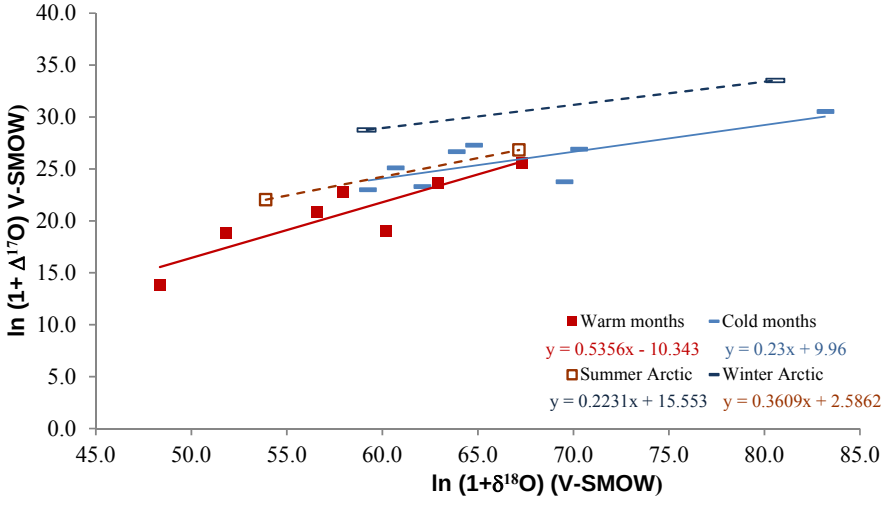

Figure 6: Isotopic results (‰) for p-NO_3^- identified by sampling periods (solid lines), compared with summer and winter trends obtained for Arctic sites (dashed lines; derived from ln (1+ δ) in Morin et al., 2008).